



---

## Figures and figure supplements

Metabolic modulation regulates cardiac wall morphogenesis in zebrafish

**Ryuichi Fukuda *et al***

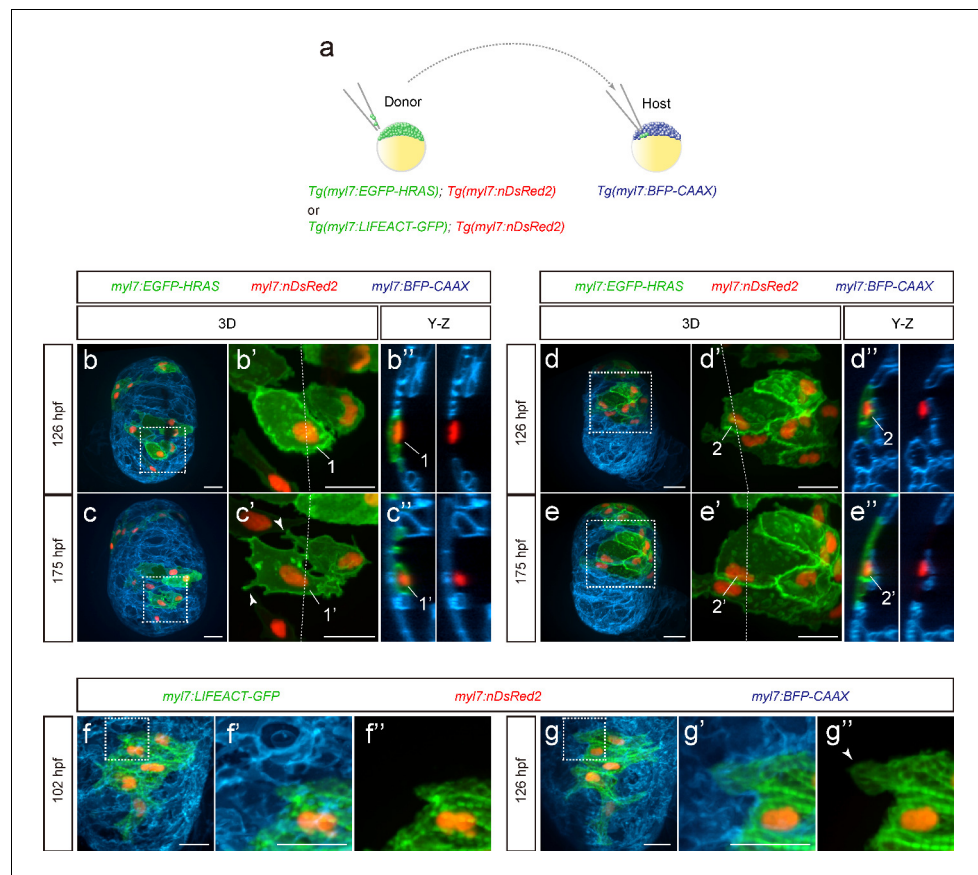


**Figure 1.** Cardiomyocyte behavior during cardiac trabeculation. (a) Schematic of the transplantation experiment. (b–e) 3D time-course images of chimeric hearts; magnified view (**b'**, **c'**, **d'**, **e'**) of area in white boxes and Y-Z plane images (**b''**, **c''**, **d''**, **e''**) along white dashed lines (**b'**, **c'**, **d'**, **e'**). CMs initially in the compact layer (**b'**, **b''**) enter the trabecular layer (**c'**, **c''**) exhibiting morphological changes and membrane protrusions (**c'**; arrowheads;  $n = 5$  CMs); CMs remaining in the compact layer (**d'**, **d''**, **e'**, **e''**) do not exhibit obvious morphological changes ( $n = 5$  CMs). The same CMs are shown at 126 and 175 hpf as indicated in the images. (f, g) 3D time-course images of chimeric heart; magnified view (**f'**, **f''**, **g'**, **g''**) of area in white boxes. CMs entering the trabecular layer exhibit partial disassembly of their sarcomeres (**g'**; arrowhead). Scale bars, 20  $\mu m$ .

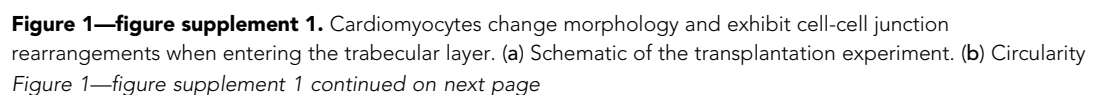


*Figure 1—figure supplement 1 continued*

analysis of CMs in the compact and trabecular layers ( $n = 7$ – $9$  CMs from 3 to 5 ventricles). (c–c'') 3D images of chimeric hearts; Y-Z plane images (d–d'') along white dashed line (c''). A host-derived CM entering the trabecular layer exhibits membrane protrusions (c, d, c', d'; arrows). (e) Schematic of the transplantation experiment. (f–f'', h–h'') 3D images of chimeric hearts; Y-Z plane images (g–g'', i–i''). A CM entering the trabecular layer exhibits N-cadherin localization in protruding membranes (g, g'; arrows), while a CM remaining in the compact layer exhibits lateral localization of N-cadherin (i, i'; arrowheads). L, cardiac lumen. Error bars, s.e.m.; \*\* $p < 0.001$  by two-tailed unpaired t-test. Scale bars, 20  $\mu\text{m}$ .

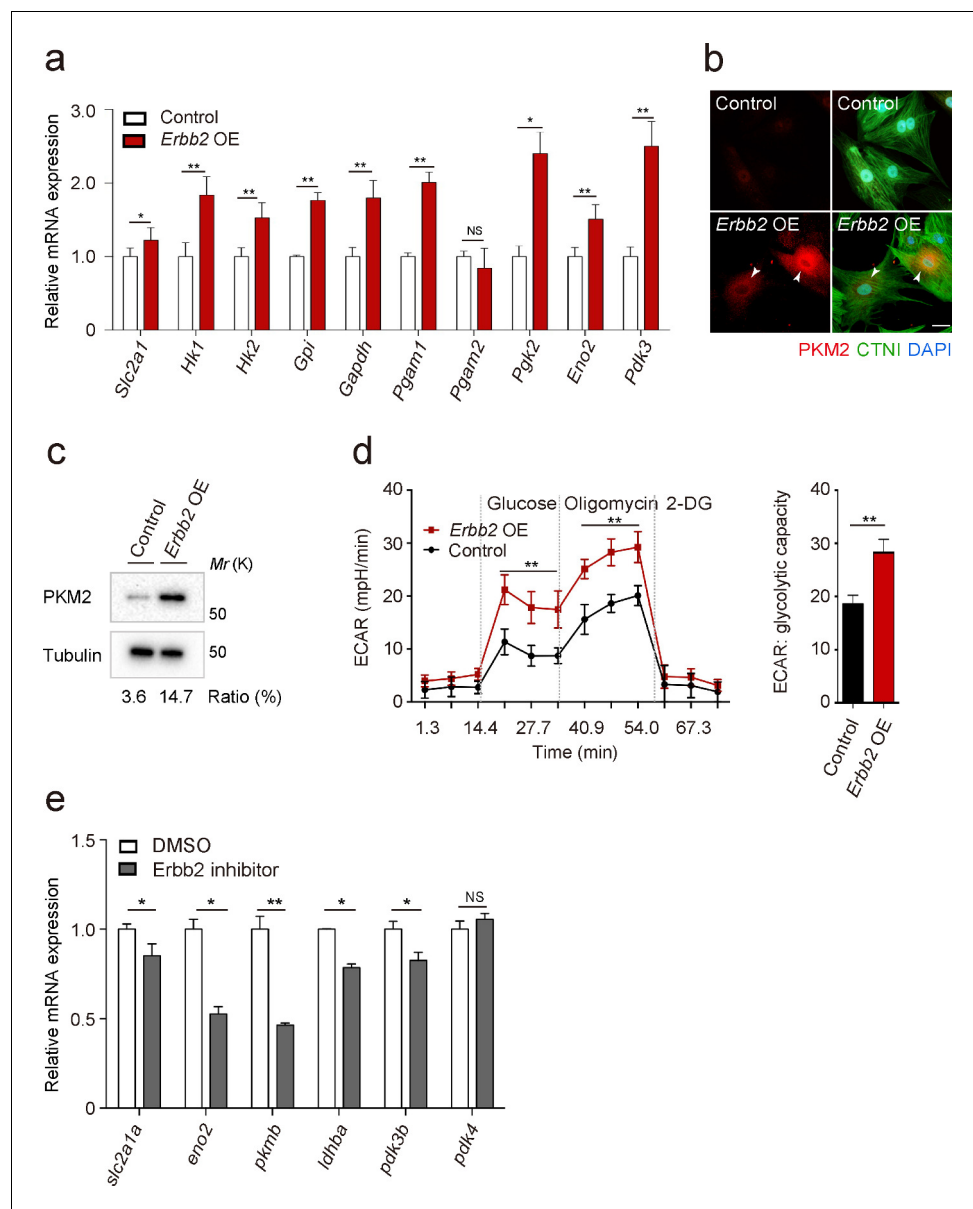


**Figure 2.** ERBB2 signaling activates glycolysis in cardiomyocytes. (a) qPCR analysis of mRNA levels of glycolytic enzyme genes in control and *Erbb2* overexpressing (OE) rat neonatal CMs ( $n = 3$ ). Error bars, s.e.m. (b) Staining for PKM2, CTNI and DNA (DAPI) in control and *Erbb2* OE rat neonatal CMs; arrowheads point to PKM2+ CMs. (c) Western blot analysis of PKM2 levels in control and *Erbb2* OE rat neonatal CMs. (d) Extracellular acidification rate (ECAR) analysis in control and *Erbb2* OE rat neonatal CMs; glycolytic capacity shown on the right ( $n = 7$ ). Error bars, s.d. (e) qPCR analysis of mRNA levels of glycolytic enzyme genes in DMSO and *Erbb2* inhibitor treated zebrafish hearts ( $n = 3$ ). Error bars, s.e.m.; \* $p < 0.05$  and \*\* $p < 0.001$  by two-tailed unpaired t-test. NS, not significant. Scale bar, 20  $\mu$ m.

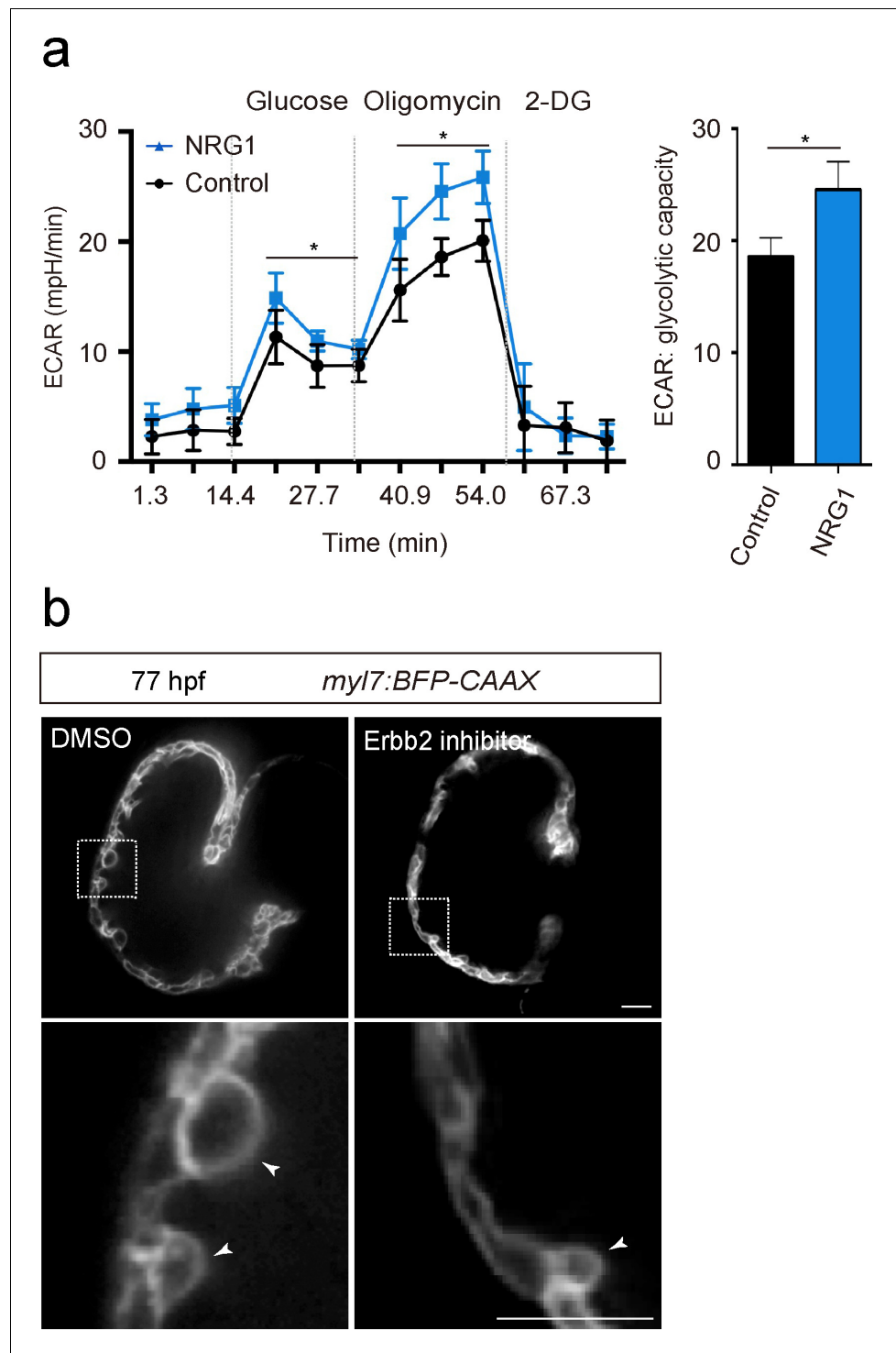


**Figure 2—figure supplement 1.** NRG1/ERBB2 signaling activates glycolysis in CMs. (a) ECAR analysis in control and NRG1 treated rat neonatal CMs; glycolytic capacity shown on the right (n = 7). (b) Confocal images (mid-sagittal sections) of 77 hpf zebrafish hearts treated with DMSO or Erbb2 inhibitor; magnified view of area in white boxes shown below; arrowheads point to CMs in the trabecular layer. Error bars, s.d.; \*p<0.05 by two-tailed unpaired t-test. Scale bars, 20 μm.

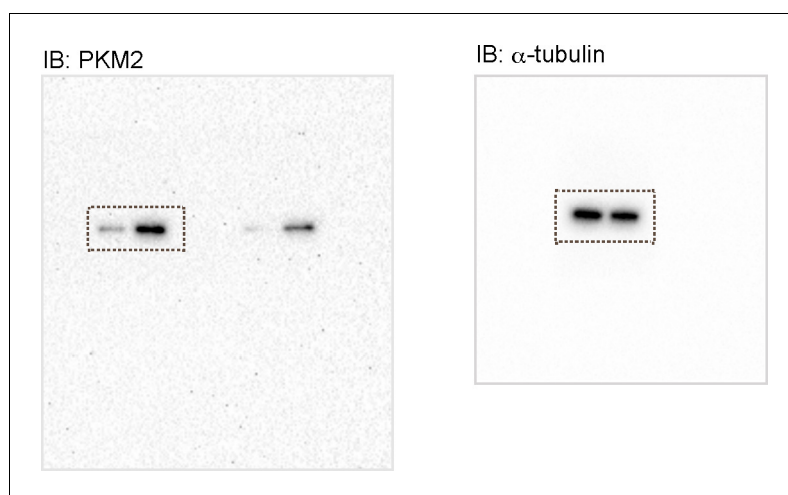


**Figure 2—figure supplement 2.** Uncropped images related to western blotting data.

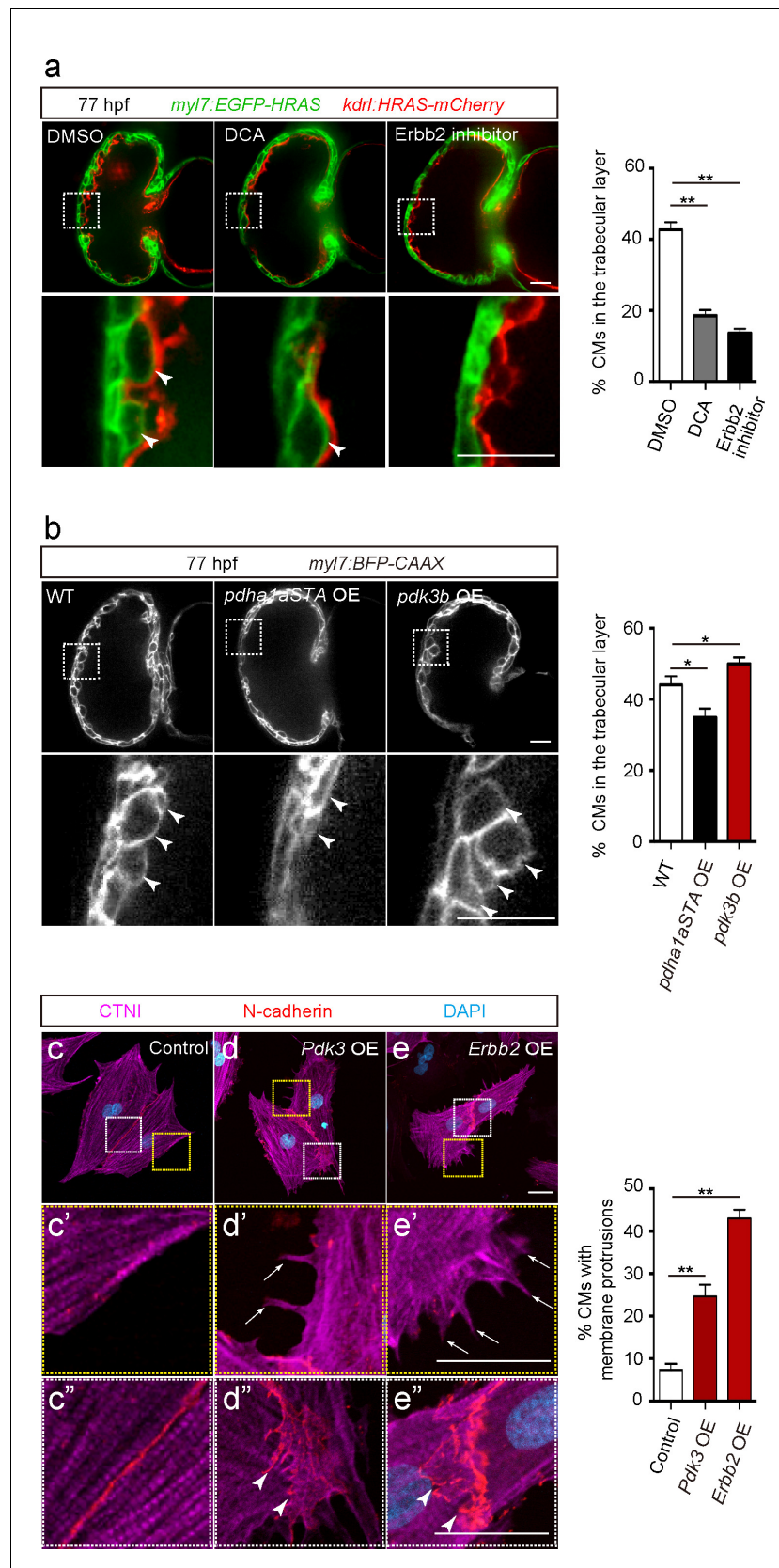


**Figure 3.** Glycolysis regulates cardiac trabeculation. (a) Confocal images (mid-sagittal sections) of 77 hpf hearts treated with DMSO, dichloroacetate (DCA) or Erbb2 inhibitor; magnified view of area in white boxes shown below; Figure 3 continued on next page



## Figure 3 continued

arrowheads point to CMs in the trabecular layer; percentage of CMs in the trabecular layer shown on the right ( $n = 5-7$  ventricles). (b) Confocal images (mid-sagittal sections) of 77 hpf *Tg(myl7:BFP-CAAX)* alone or in combination with *Tg(myl7:pdha1aSTA-P2A-tdTomato)* or *Tg(myl7:pdk3b-P2A-tdTomato)* hearts; magnified view of area in white boxes shown below; arrowheads point to CMs in the trabecular layer; percentage of CMs in the trabecular layer shown on the right ( $n = 5-7$  ventricles). (c–e”) Staining for CTNI, N-cadherin and DNA (DAPI) in control (c), *Pdk3* (d) and *ErbB2* (e) OE rat neonatal CMs; magnified view of area in yellow (c’, d’, e’) and white (c”, d”, e”) boxes; percentage of CMs exhibiting membrane protrusions shown on the right ( $n = 3$  individual experiments; each value corresponds to an average of 30 CMs). *Pdk3* and *ErbB2* OE causes rat neonatal CMs to exhibit membrane protrusions (d’, e’; arrows) and cell-cell junction rearrangements (d’, e’; arrowheads). Error bars, s.e.m.; \* $p < 0.05$  and \*\* $p < 0.001$  by ANOVA followed by Tukey’s HSD test. Scale bars, 20  $\mu\text{m}$ .

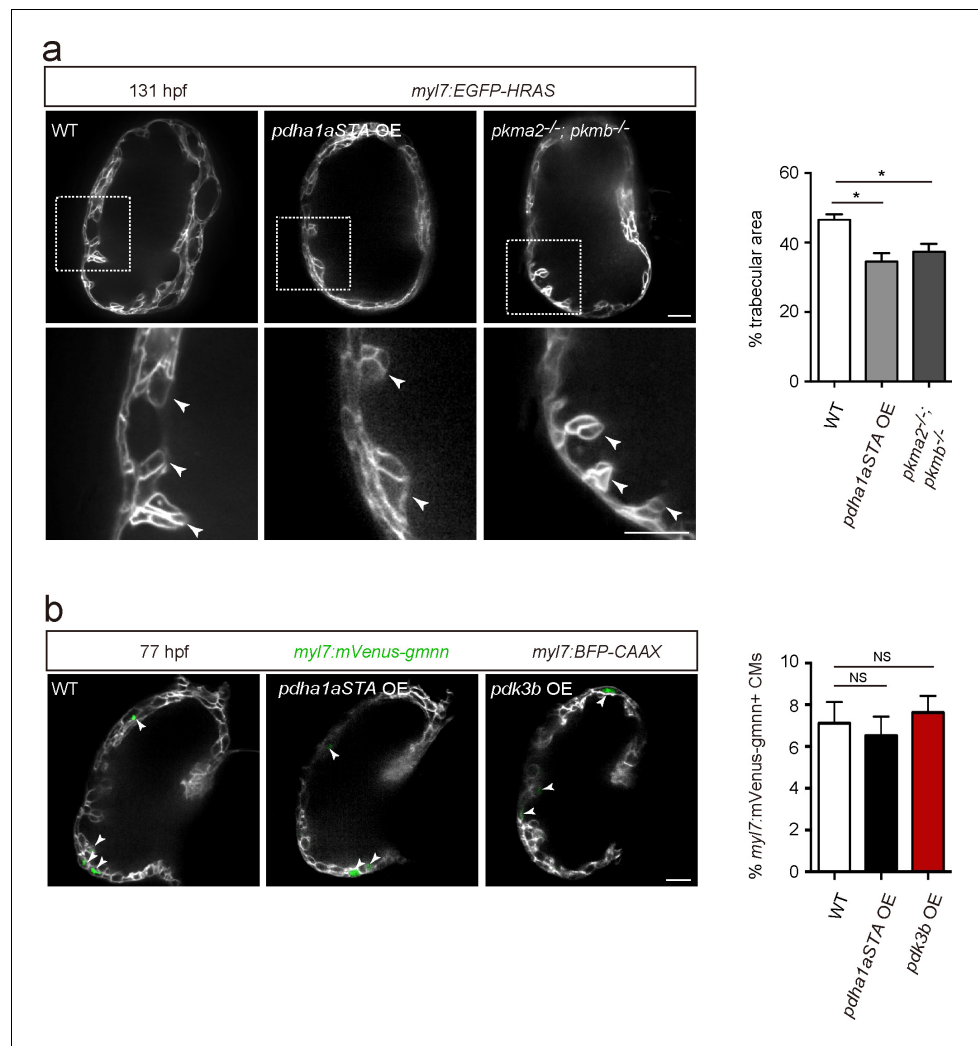


**Figure 3—figure supplement 1.** Cardiomyocyte proliferation does not appear to be affected by modulation of glycolysis. (a) Confocal images (mid-sagittal sections) of 131 hpf *Tg(myl7:EGFP-HRAS)* alone or in combination with *Tg(myl7:pdha1aSTA-P2A-tdTomato)* and of 131 hpf *Tg(myl7:EGFP-HRAS); pkma2<sup>-/-</sup>; pkmb<sup>-/-</sup>* hearts; magnified view of area in white boxes shown below; arrowheads point to trabecular CMs; percentage of trabecular area shown on the right ( $n = 5$  ventricles). (b) Confocal images (mid-sagittal sections) of 77 hpf *Tg(myl7:mVenus-gmnn)*; *Tg(myl7:BFP-CAAX)* alone or in combination with *Tg(myl7:pdha1aSTA-P2A-tdTomato)* or *Tg(myl7:pdk3b-P2A-tdTomato)* hearts; arrowheads point to *myl7:mVenus-Gmnn*+ CMs; percentage of *myl7:mVenus-Gmnn*+ CMs shown on the right ( $n = 5$  ventricles). Error bars, s.e.m.; \* $p < 0.05$  and \*\* $p < 0.001$  by two-tailed unpaired t-test (a) or ANOVA followed by Tukey's HSD test (b). NS, not significant. Scale bars, 20  $\mu$ m.

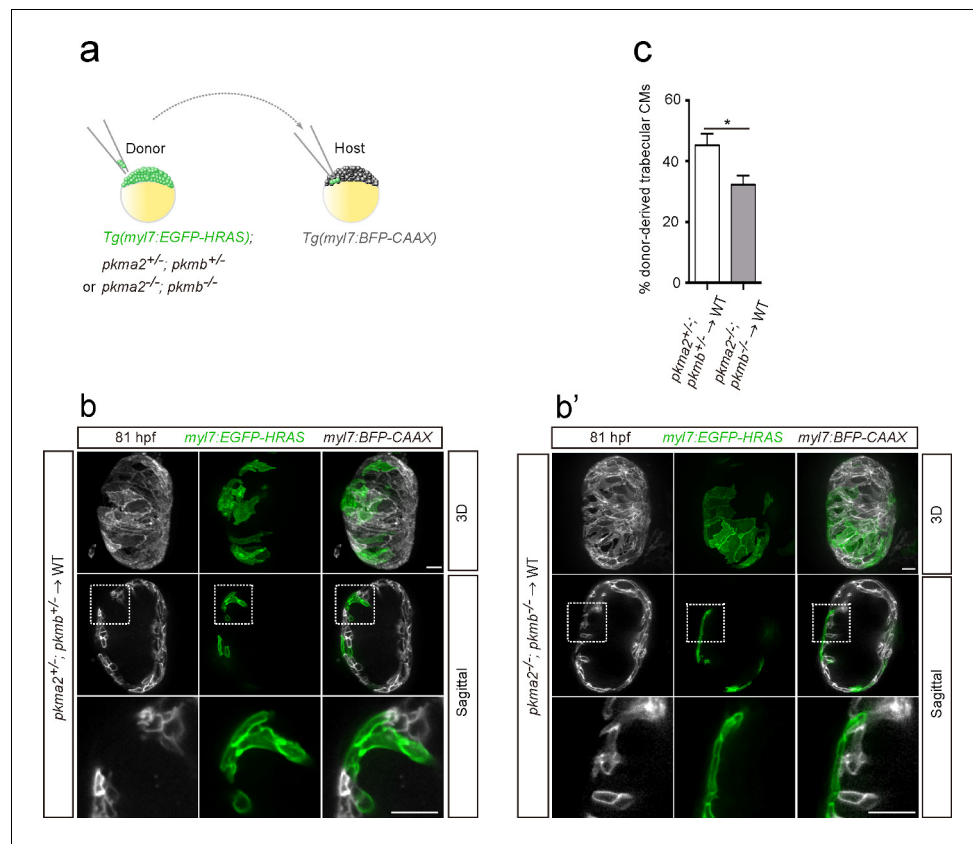


**Figure 4.** Loss of *pkm2* impairs cardiac trabeculation. (a) Schematic of the transplantation experiment. (b, b') 3D and mid-sagittal section images of chimeric hearts using *pkm2<sup>+/-</sup>; pkmb<sup>+/-</sup>; Tg(myl7:EGFP-HRAS)* (b) and *pkm2<sup>-/-</sup>; pkmb<sup>-/-</sup>; Tg(myl7:EGFP-HRAS)* (b') cells as donors; magnified view of area in white boxes shown below. (c) Percentage of donor-derived trabecular CMs ( $n = 10$  ventricles). Error bars, s.e.m.; \* $p < 0.05$  by two-tailed unpaired  $t$ -test. Scale bars, 20  $\mu$ m.

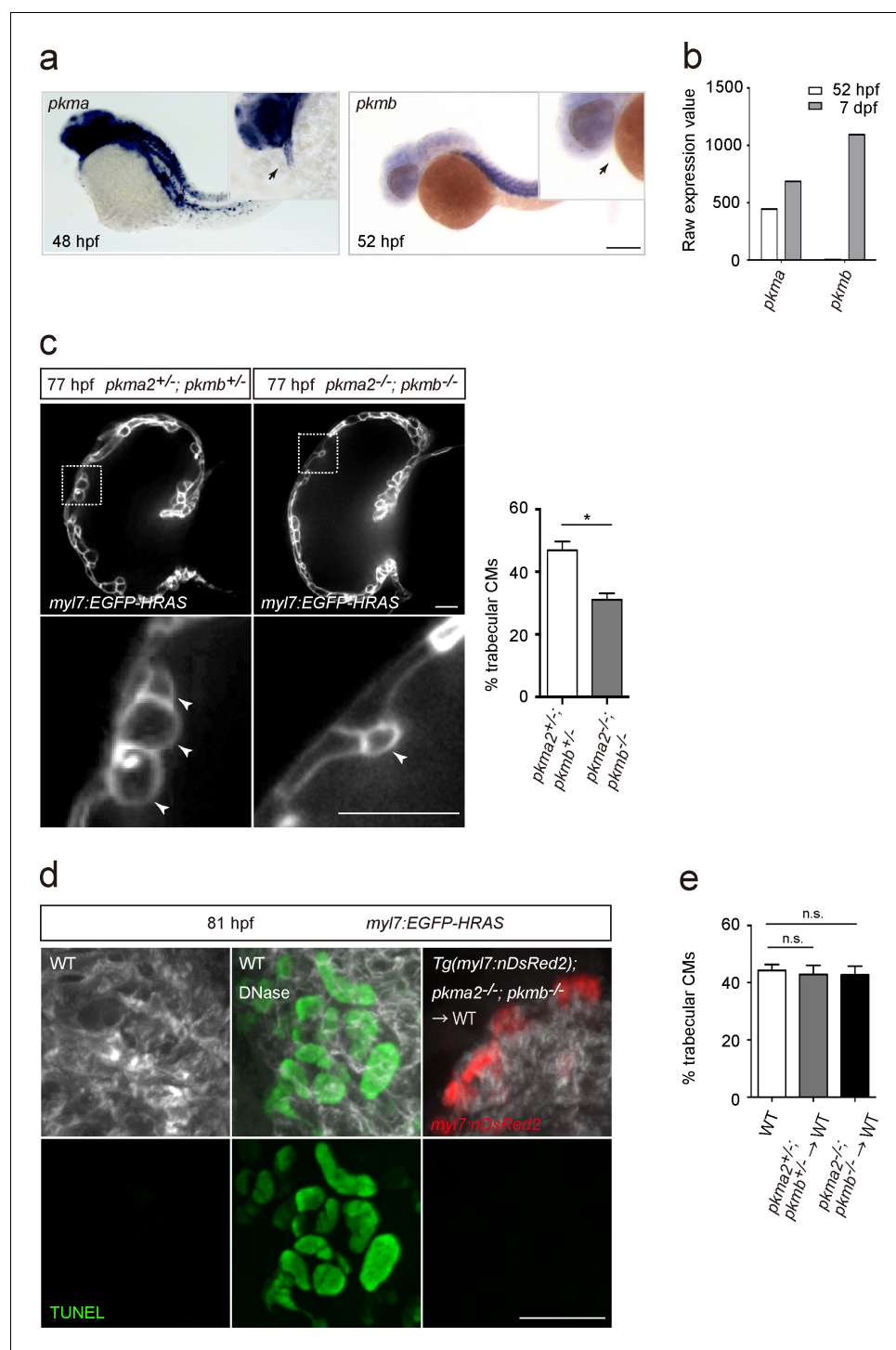


**Figure 4—figure supplement 1.** Glycolytic enzymes regulate cardiac trabeculation. (a) Analysis of *pkma* and *pkmb* mRNA expression by in situ hybridization; magnified view shown in the top right corner; arrows point to the heart. (b) Expression levels of *pkma* and *pkmb* in 52 hpf and seven dpf hearts as detected by microarray analysis. (c) Confocal images (mid-sagittal sections) of 77 hpf *Tg(my17:EGFP-HRAS); pkma2*<sup>+/−</sup>; *pkmb*<sup>+/−</sup> and *Tg(my17:EGFP-HRAS); pkma2*<sup>−/−</sup>; *pkmb*<sup>−/−</sup> hearts; magnified view of area in white boxes shown below; arrowheads point to CMs in the trabecular layer; percentage of CMs in the trabecular layer shown on the right ( $n = 5$ –7 ventricles). (d) TUNEL assay in WT and chimeric hearts using *Tg(my17:nDsRed2); pkma2*<sup>−/−</sup>; *pkmb*<sup>−/−</sup> cells as donors. As a positive control for the TUNEL assay, WT embryos were treated with DNase. (e) Percentage of trabecular CMs in WT and chimeric hearts using *pkma2*<sup>+/−</sup>; *pkmb*<sup>+/−</sup> or *pkma2*<sup>−/−</sup>; *pkmb*<sup>−/−</sup> cells as donors ( $n = 5$  ventricles). Error bars, s.e.m.; \* $p < 0.05$  by Figure 4—figure supplement 1 continued on next page

Figure 4—figure supplement 1 continued

two-tailed unpaired t-test (c) or ANOVA followed by Tukey's HSD test (e). Scale bars, 200  $\mu\text{m}$  in a; 20  $\mu\text{m}$  in c and d.